

Applications of radar interferometry for measuring ice motion

Dyre Oliver Dammann¹, Andrew R. Mahoney¹, Mark Johnson², Hajo Eicken³, Leif E.B. Eriksson⁴, Franz J. Meyer¹, Emily Fedders¹, Mark Fahnestock¹

¹ Geophysical Institute, University of Alaska Fairbanks, Fairbanks, Alaska, USA

² College of Fisheries and Ocean Sciences, University of Alaska Fairbanks, AK, USA

³ International Arctic Research Center, University of Alaska Fairbanks, Fairbanks, AK, USA

⁴ Chalmers University of Technology, Gothenburg, Sweden

ABSTRACT

Ongoing sea ice decline has major implications for human activities near sea ice due to shorter seasons for on-ice operations and thinner ice with reduced load-bearing capacity and stability in many regions. This may in turn lead to increased sea ice mobility and impacts of ice movement on structures. We investigate space-borne radar interferometry (InSAR) as a technique to measure mm-scale sea ice motion of stationary ice over weeks to months. We find that InSAR enables mapping of bottomfast and stabilized landfast ice as regions with near-zero or reduced deformation. We further use this data to derive landfast ice strain and stress enabling estimation of the fracturing potential along the Northstar Island ice road in the Beaufort Sea, Alaska. We further examine ground-based radar interferometry (GRI) as a tool to collect continuous near real-time measurements on the km-scale not possible with InSAR. Based on GRI measurements conducted in Utqiagvik, Alaska, we demonstrate the ability to evaluate ice strain in stationary ice and track vertical ice displacement due to tides. We also collected GRI measurements at 500 Hz during a drifting ice camp in the Beaufort Sea. The high sampling rate enabled tracking of continuous strain and detection of subtle variations in behavior between ice regimes. Through this work, interferometry shows promise as a tool to observe ice motion at the relevant scales needed for assessing sea ice stability, identify precursors to failure events, and better understand the relationship between different ice properties and loads on structures.

KEY WORDS Remote sensing, Ice-structure interactions; Ice roads; Sea ice; Ice strain.

INTRODUCTION

Over the last fifty years, transportation and resource extraction have led to increased human presence in the Arctic and further diversification of ice use (Eicken et al., 2009). During the same time period, Arctic sea ice has declined substantially leading to an increasingly open Arctic Ocean during summer (Comiso et al., 2017). Such changes can ease navigation (Stephenson et al., 2011), but can also increase hazards as earlier break-up of coastal ice can result in larger advection of multiyear ice into shipping lanes (Barber et al., 2018). Sea ice decline can result in thinner and more dynamic sea ice (Spreen et al., 2011) with implications for stability and fracturing (Rampal et al., 2009). This can have implications for maritime activities and ice as a hazard, which play a prominent role in offshore resource development (Eicken and Mahoney, 2015). This is particularly relevant for coastal sea ice due to the broad range of human reliance on stationary landfast ice (Eicken et al., 2009) and the role of sea ice hazards in development of coastal infrastructure (Eicken and Mahoney, 2015).

Due to the relevance of sea ice for operations and its role in Arctic change, there is a need to be able to quantify sea ice motion relevant to strategic planning and operational support of operations. There is also a need to better understand ice motion from the perspective of loads on structures and destabilization and fracturing relevant to strategic planning of operations. Numerous approaches exist for quantifying ice motion including GPS buoys (Zhang et al., 2003) and high-precision sensors such as ice stress buoys and accelerometers (Johnson et al., 2020). However, such sensors are limited to point-based observations and require the deployment of equipment on the ice. Space-borne systems can provide data over large spatial extent for mapping of stationary ice using optical sensors (Fraser et al., 2020) and deriving drift based on passive microwave systems (Spreen et al., 2011) with a low km-scale resolution.

Radar systems are capable of providing m-scale resolution to support operations regardless of weather and light conditions. Space-borne synthetic aperture radar (SAR) can be used to map stationary ice (Mahoney et al., 2014) and derive km-scale ice motion products (Berg and Eriksson, 2014). However, the temporal sampling is low with scenes typically acquired hours to days apart. In coastal areas, shore-based radar systems can be used to obtain higher minute-scale temporal sampling (Jones et al., 2016), but systems are sparse and limited to coastal waters. Systems are also limited to evaluate m-scale motion, which is valuable for tracking drift or detecting large-scale deformation events. However, they typically cannot be used to resolve mm- to cm-scale deformation leading to fracturing or destabilization of stationary ice.

Radar interferometry is a technique that evaluates the phase information in radar signals which is sensitive to mm-scale motion. This enables InSAR to resolve dynamic processes relevant to fracture and destabilization of ice that are difficult to evaluate with other techniques over the same spatial scale (Berg et al., 2015). Applications of InSAR are typically limited by data availability. However, analysis can potentially be improved by utilizing ground-based interferometric radars (GRI) such as the Gamma Portable Radar Interferometer (GPRI) (Figure 1) (Werner et al., 2012). Here, we aim to give an overview over our recent work with InSAR and GRI relevant to operations.



Figure 1. The Gamma Portable Radar Interferometer (GPRI) mounted on a multiyear ice ridge in the Beaufort Sea during a field campaign in 2020.

RADAR INTERFEROMETRY

A radar system emits a propagating electromagnetic wave signal. Conventional radar applications are based on analysis of the amplitude (i.e., strength) of the signal that scatters back from objects within the radar footprint. Interferometry is a technique that evaluates how the phase of the returning electromagnetic wave changes over time. If the scattering object moves closer or further from the radar, the return radar signal will have a slightly different phase value, which is proportional to line-of-sight (LOS) motion. An interferogram is a spatial representation of the phase change between two acquisitions with phase values ranging between 0 and 360 degrees. In the case of m-scale motion, phase values will “wrap around” from 360 and back to 0 resulting in ambiguous phase values. Interferograms therefore often appear as stripes (known as fringes) of equal phase values, where increasingly denser fringes are indicative of larger changes in relative motion (i.e., deformation). Data from different coherent radar systems and observation setups can be processed for interferometry including synthetic aperture radar (SAR) and ground-based radar illustrated in Figure 2.

Synthetic Aperture Radar Interferometry (InSAR)

InSAR requires two or more SAR scenes obtained from a similar viewing geometry and no more than a few meters of ice motion (depending on resolution) during the time lag between acquisitions. There are two general types of InSAR applicable to sea ice known as repeat-pass and single-pass. Repeat-pass InSAR utilizes scenes from different overpasses of the same satellite. The orbit repeat time thus represents the temporal lag between acquisitions. This ranges from days to weeks and represents the time interval over which the InSAR-derived motion is averaged. Many current and past SAR systems can be processed for repeat-pass interferometry, including Japanese ALOS PALSAR and the European Sentinel-1, whose data we utilize here (see “A” in Figure 2). However, due to the time to complete an orbit cycle, repeat-pass InSAR is only applicable to stationary ice. Single-pass interferometry also utilizes two acquisitions, but from different satellites in close proximity of one another. This can significantly reduce the temporal lag enabling derivation of sea ice drift speed (see “B” in Figure 2). However, currently only the German TanDEM-X constellation enables this application.

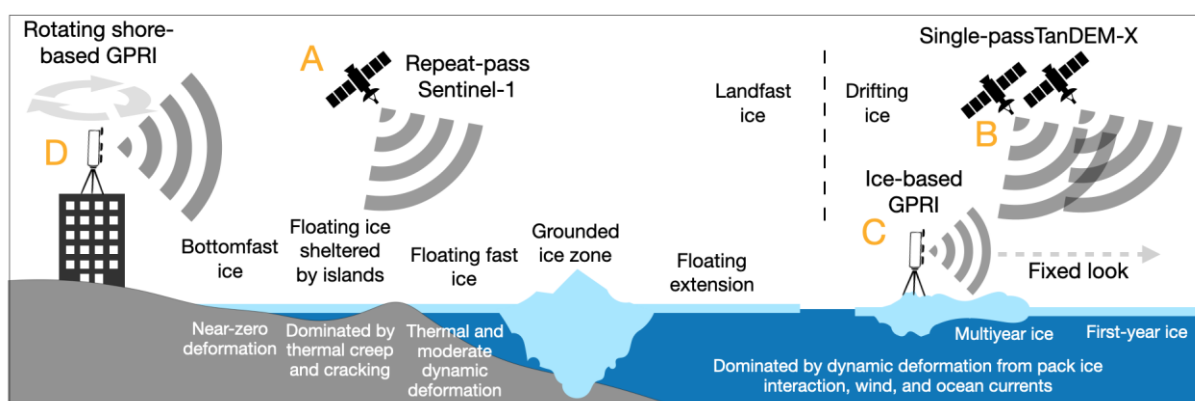


Figure 2. Schematic of different dynamic ice regimes including landfast and drifting ice. Letters A-D indicate example acquisition geometries discussed in the text.

Ground-based radar interferometry (GRI)

While SAR scenes are typically acquired with a fixed look angle from a moving platform, a ground-based system can rotate while scanning the surface. The GPRI obtains LOS sea ice

motion out to a ~5 km radius. A full near 360°-degree repeat-scan interferogram can be constructed from two scans with a temporal lag ranging from days and down to ~ 3 minutes (i.e. time to complete a full scan). If using partial scans of a small sector, the temporal lag can potentially be reduced to less than a minute. Sampling rate can be enhanced substantially and potentially up to 500 Hz (Werner et al., 2012) if the GPRI look angle is kept fixed. This is referred to as stare-mode interferometry which enables interferogram formation with temporal lags between acquisitions down to 2 ms for the derivation of near instantaneous motion. We analyze one 30 s stare-mode interferogram acquired during a field campaign on drifting Beaufort Sea ice on 3 March 2020 (Figure 1; see “C” in Figure 2). We also examine over 250 6-minute repeat-scans acquired between 00:55 UTC to 23:04 UTC on 16 May 2012 in Utqiagvik, Alaska, not previously analyzed.

RESULTS

InSAR-based evaluation of ice stability and fracture potential over days

We examined multiple interferograms from Sentinel-1A and B satellites during April-May 2017 over the Beaufort Sea coastline of Alaska (Figure 3a). Here, the extent of the colored fringes marks the extent of landfast ice (Meyer et al., 2011). We also notice that the fringes are either widely spaced (smaller deformation) or tightly spaced (larger deformation) which depends on the extent of sea ice grounding. Grounded ridges constrain shoreward motion of the ridge due to the frictional coupling with the sea floor (Figure 2). Thus lines of grounded ridges tend to exhibit a stark gradient in fringe spacing (Figure 3a) (Dammann et al., 2019a). We can further discriminate level bottomfast sea ice due to the lack of interferometric phase change as bottomfast ice experiences near zero deformation (Dammann et al., 2018b) (Figure 2). As an example, we can identify the boundary of bottomfast ice along the Oooguruk Island ice road in the Colville Delta, Alaska (Figure 3b). Through InSAR, we determined that part of the ice road spans across floating ice, while the end sections are grounded. We further demonstrated how InSAR enables pan-Arctic scale evaluation of sea ice stability zones (Dammann et al., 2019a) (Figure 3c).

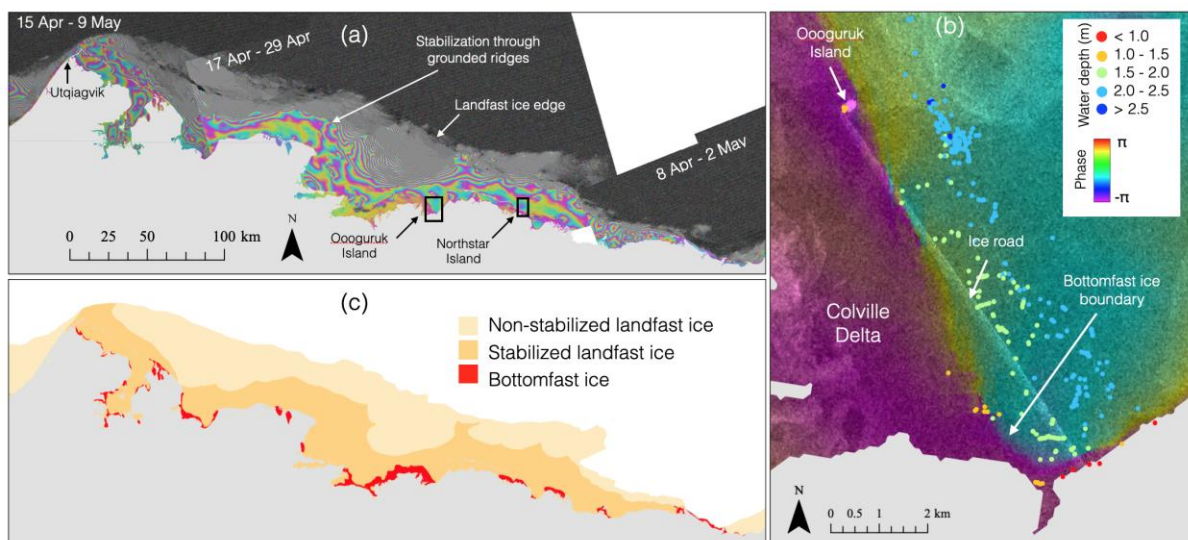


Figure 3. (a) Sentinel-1 interferograms over the Beaufort Sea coast of Alaska during April-May 2017. (b) Overlaid backscatter and interferogram along the Oooguruk Island ice road (black rectangle in (a)), indicating areas of bottomfast ice underneath the ice road. (c) Landfast ice dynamic regimes based on (a).

Through the interferometric phase, we can quantify ice deformation (Dammann et al., 2016). We demonstrated this approach near the Northstar Island ice road near Prudhoe Bay, Alaska (black rectangle in Figure 3a; Figure 4a). The analysis is based on two ALOS PALSAR acquisitions 46 days apart. The InSAR-derived motion enabled the derivation of stress using an elastic rheology model (Figure 4b) (Dammann et al., 2018a). The stress exhibit values far exceeding the expected yield stress resulting in estimated brittle fracture density (Figure 4c). There are uncertainties surrounding the exact number of fracturing events. However, the relative fracture density near the road (Figure 4d) can potentially aid allocation of ground-survey resources. We found here that the middle section of the road is deforming at relatively high rate. This is consistent with a known fracturing problem surrounding mile point 4.3 (Figure 4d) and pre-deformed ice (Figure 4a) (Dammann et al., 2018a).

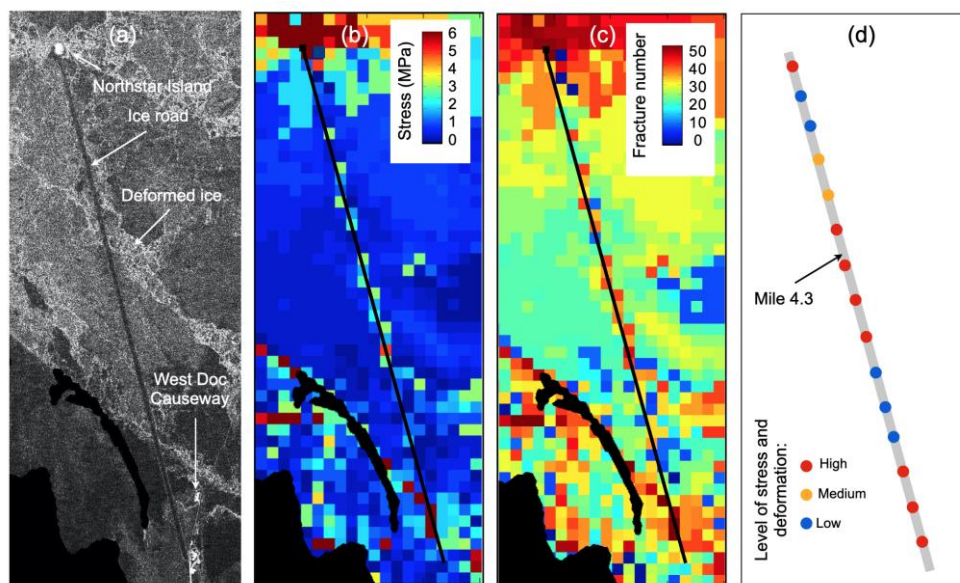


Figure 4. (a) ALOS PALSAR backscatter imagery on 21 Mar 2010 near the Northstar Island ice road. (b) Derived hypothetical elastic tensile stress derived from an interferogram between 21 Mar and 6 May 2010. (c-d) Estimated and relative fracture density.

GRI-based tracking of sub-hourly changes in landfast ice displacement

The analysis above is based on average motion over several days to months. We also explored the potential for higher interferometric sampling using a GPRI to evaluate how landfast ice deformation and displacement changes over time. We acquired 22 hours of repeat-scan data from a radar placed on top of a building in Utqiagvik, Alaska, during predominately offshore winds. We evaluated the displacement of six points on a line near directly offshore from the GPRI (Figure 5a). Within a few hundred meters of the sensor, the phase is sensitive to vertical as well as lateral ice motion (Dammann et al., 2021). Close to the grounded ridge at 800 m, we interpret the ice motion as vertical as we expect the ridge to constrain lateral offshore motion (Figure 5b). The vertical displacement matches well with tidal amplitudes predicted by the National Oceanic and Atmospheric Administration (NOAA) tide model (red crosses in Figure 5b). We assume uniform vertical displacements across the scene enabling the removal of the same vertical contribution from the interferometric phase change at all control points (Figure 5c). This indicates increasing offshore motion in response to an increase in wind speed (gray line in Figure 5c). Here, the points furthest from the ridge move the most as they have the most area over which the ice can compress shoreward of the ridge or stretch offshore (Dammann et al., in prep).

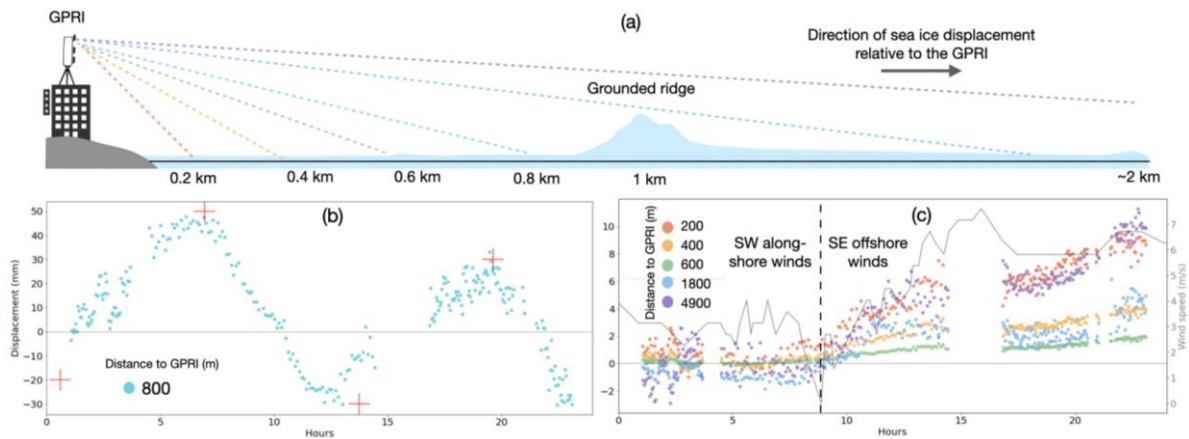


Figure 5. (a) Acquisition geometry of shore-based GPRI data collection in Utqiagvik. (b) Progressive vertical ice displacement closely matching the tidal cycle. (c) Horizontal compressional and divergent ice motion on each side of the grounded ridge.

InSAR- and GRI-derived instantaneous motion and deformation of drifting ice

The analysis above evaluates interferograms with temporal lags, and average derived motion, of several minutes. Using TanDEM-X InSAR, it is possible to derive near instantaneous motion (averaged over 10 ms). We demonstrate this technique with an interferogram of the Vilkitsky Strait along the Northern Sea Route. The westerly winds and ice motion lead to open water on the east side of Cape Chelyuskin (Figure 6a), allowing otherwise confined ice to move more freely. The derived instantaneous motion is indicative of multiple dynamic regimes including stationary ice near the coastlines (A) and a central channel (C) with faster flow than a transition zone towards the landfast ice (B) (Figure 6b). The central channel features variable speed and a convergence discontinuity extending northward from Cape Chelyuskin. This example illustrates how interferometry can be used to distinguish between different dynamic regimes and short-lived transient dynamic processes not detectible with other methods (Dammann et al., 2019b). Such work is of particular interest in locations such as Vilkitsky Strait where formation of ice arches results in a major choke point along the Northern Sea Route, requiring heavy icebreaker assistance for vessels transiting the strait.

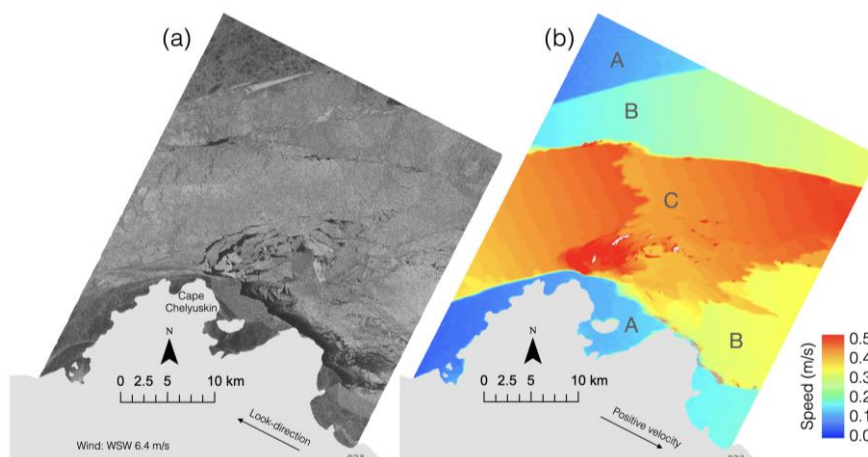


Figure 6. (a) TanDEM-X backscatter scene over Vilkitsky Strait 17 Dec 2013. (b) InSAR-derived LOS motion. Land is masked out in light gray.

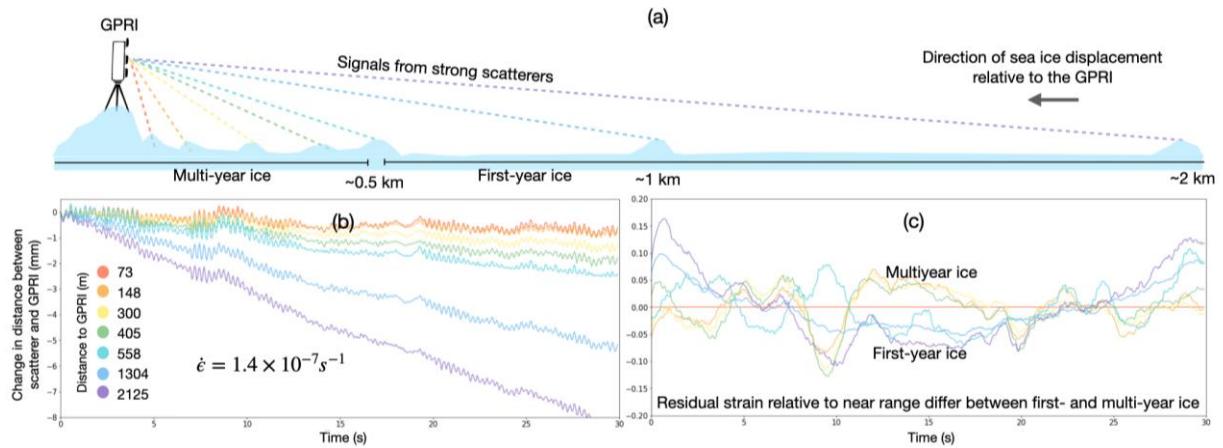


Figure 7. (a) Acquisition geometry of GPRI data collection on drifting ice in the Beaufort Sea. (b) Progressive lateral ice deformation indicative of uniform convergent strain. (c) Residual strain exhibits different dynamics between first- and multi-year ice.

The use of InSAR-derived instantaneous motion is limited by sparse data availability. We thus explored the potential for higher sampling using GPRI to evaluate ice deformation and displacement changes over time. We deployed a GPRI on drifting sea ice during a field campaign in the Beaufort Sea (Figure 1; see “C” in Figure 2). The GPRI was placed on a multiyear ridge starting in a fixed direction towards smoother first-year ice (Figure 7a). We further evaluated the deformation over time relative to the GPRI at seven points on the ice. During 30 s, the ice uniformly converges towards the GPRI with a strain rate of $1.4 \times 10^{-7} \text{ s}^{-1}$ (Dammann et al., 2021). We removed the convergence trend and derived the residual deformation (Figure 7c). This reveals a slightly different ice motion of the multiyear and first-year ice on the sub-mm scale likely due to different ice properties such as thickness, porosity and preexisting microfractures.

CONCLUSIONS

In this work, we summarized different applications of radar interferometry for evaluating sea ice motion with potential relevance to operations on or near sea ice. This is based on previously published work with InSAR as well as recent unpublished work with GPRI. We examined the use of InSAR to map sea ice based on stability and found that InSAR can enable the discrimination of bottomfast sea ice. This is relevant for over-ice transport due to the near infinite load-bearing capacity of bottomfast sea ice in comparison with floating ice. We demonstrate this with *in-situ* validation depth measurements near Oooguruk Island, Alaska, a man-made island constructed from materials transported strictly across bottomfast sea ice.

We also found that we are able to map ice that is stabilized by grounded ridges. This is relevant to on-ice operations as grounded ridges are frictionally coupled to the sea floor and hamper lateral motion during forcing events. Landfast ice shoreward of grounded ridges are thus in many regions associated with reduced risk of breakouts. We further demonstrated the ability of InSAR to quantify average motion over days to weeks to derive of landfast ice strain and estimate internal stress. This enables the assessment of destabilization through fracturing possibly reducing tensile yield stress and load-bearing capacity.

The data availability of InSAR is limited, which places constraints on the use of this technique, in particular as it does not enable evaluation of motion over shorter timespans in between acquisitions. We here demonstrated that GPRI can be used locally to track the development of

sea ice strain over shorter timespans of minutes. If placed on shore, this can enable the near real-time tracking of vertical ice displacement as a result of tides and or surges. This has potential relevance for operations in areas of substantial tidal movements or for tracking impacts of tides on ice near grounded ice or structures. We also demonstrated how the GPRI can track lateral ice motion in response to offshore winds which can lend key insight into what ridges are grounded. It can also provide insight into the rheological behavior of floating ice and the possibility of fracturing and destabilization of coastal sea ice.

We demonstrated how the GPRI can be applied in stare mode to derive instantaneous motion similar to TanDEM-X interferometry. This can be used to evaluate progression of strain rate during deformation and evaluate dynamic differences across the ice. The high mm-scale accuracy and 500 Hz sampling rate may also have significant applications for examining the role of drift speed on loads on structures under different conditions.

We find that radar interferometry enables the assessment of both landfast and drifting sea ice dynamics with an unmatched combination of spatial coverage and accuracy. The combination of InSAR with GRI can also locally reduce the temporal constraints of InSAR. There is a need to further investigate how to combine InSAR and ground-based interferometry and incorporate approaches into operational workflows.

ACKNOWLEDGEMENTS

This work was partly funded by the Seasonal Ice Zone observing Network (NSF-0856867), the Swedish National Space Agency (Dnr. 192/15), and the Office of Naval Research SIDEx program (N000142MP001). ALOS PALSAR data was provided by the Alaska Satellite Facility (ASF) through an ALOS data grant from the JAXA. TanDEM-X data were provided free of charge by DLR through a science proposal (XTI_GLAC6921). Sentinel-1 data are provided free of charge by the European Union Copernicus program and were accessed through ASF.

REFERENCES

- Barber, D., Babb, D., Ehn, J., Chan, W., Matthes, L., Dalman, L., Campbell, Y., Harasyn, M., Firoozy, N., and Theriault, N.: Increasing mobility of high Arctic sea ice increases marine hazards off the east coast of Newfoundland, *Geophys Res Lett*, 45, 2370-2379, 10.1002/2017GL076587, 2018.
- Berg, A., and Eriksson, L. E. B.: Investigation of a hybrid algorithm for sea ice drift measurements using synthetic aperture radar images, *IEEE Transactions on Geoscience and Remote Sensing*, 52, 5023-5033, 2014.
- Berg, A., Dammert, P., and Eriksson, L. E. B.: X-Band Interferometric SAR Observations of Baltic Fast Ice, *IEEE Transactions on Geoscience and Remote Sensing*, 53, 1248-1256, 10.1109/TGRS.2014.2336752, 2015.
- Comiso, J. C., Meier, W. N., and Gersten, R.: Variability and trends in the Arctic Sea ice cover: Results from different techniques, *Journal of Geophysical Research: Oceans*, 122, 6883-6900, 2017.
- Dammann, D. O., Eicken, H., Meyer, F., and Mahoney, A.: Assessing small-scale deformation and stability of landfast sea ice on seasonal timescales through L-band SAR interferometry and inverse modeling, *Remote Sens Environ*, 187, 492-504, 10.1016/j.rse.2016.10.032, 2016.
- Dammann, D. O., Eicken, H., Mahoney, A., Meyer, F., Freymueller, J., and Kaufman, A. M.: Evaluating landfast sea ice stress and fracture in support of operations on sea ice using SAR interferometry, *Cold Reg Sci Technol*, 10.1016/j.coldregions.2018.02.001, 2018a.
- Dammann, D. O., Eriksson, L. E. B., Mahoney, A., Stevens, C. W., Van der Sanden, J., Eicken,

H., Meyer, F., and Tweedie, C.: Mapping Arctic bottomfast sea ice using SAR interferometry, *Remote Sensing*, 10(5), 720, 10.3390/rs10050720, 2018b.

Dammann, D. O., Eriksson, L. E., Mahoney, A. R., Eicken, H., and Meyer, F. J.: Mapping pan-Arctic landfast sea ice stability using Sentinel-1 interferometry, *The Cryosphere*, 13, 557-577, 10.5194/tc-13-557-2019, 2019a.

Dammann, D. O., Eriksson, L. E. B., Jones, J. M., Romeiser, R., Mahoney, A. R., and Fukamachi, Y.: Instantaneous sea ice drift speed from TanDEM-X interferometry, *The Cryosphere*, 10.5194/tc-2018-242, 2019b.

Dammann, D. O., Johnson, M. A., Fedders, E., Mahoney, A., Werner, C., Polashenski, C. M., Meyer, F., and Hutchings, J. K.: Ground-based radar interferometry of sea ice, *Remote Sensing*, 13(1), 10.3390/rs13010043, 2021.

Dammann, D. O., Johnson, M. A., Mahoney, A., Ito, M., Hutchings, J. K., Fedders, E., and Polashenski, C. M.: Monitoring tide- and wind-driven landfast sea ice dynamics with ground-based radar interferometry, *Cold Reg Sci Technol*, 10.3390/rs13010043, in prep.

Eicken, H., Lovecraft, A. L., and Druckenmiller, M. L.: Sea-Ice System Services: A Framework to Help Identify and Meet Information Needs Relevant for Arctic Observing Networks, *Arctic*, 62, 119-136, 10.14430/arctic126, 2009.

Eicken, H., and Mahoney, A. R.: Sea Ice: Hazards, Risks, and Implications for Disasters, in: *Coastal and Marine Hazards, Risks, and Disasters*, edited by: Ellis, J. T., Sherman, D. J., and Shroder, J. F., Elsevier Inc., Amsterdam, Netherlands, 381-399, 2015.

Fraser, A. D., Massom, R. A., Ohshima, K. I., Willmes, S., Kappes, P. J., Cartwright, J., and Porter-Smith, R.: High-resolution mapping of circum-Antarctic landfast sea ice distribution, 2000–2018, *Earth System Science Data Discussions*, 1-18, 2020.

Johnson, M., Mahoney, A., Sybrandy, A., and Montgomery, G.: Measuring acceleration and short-lived motion in landfast sea-ice, *Journal of Ocean Technology*, 15, 2020.

Jones, J. M., Eicken, H., Mahoney, A. R., Rohith, M. V., Kambhamettu, C., Fukamachi, Y., Ohshima, K. I., and George, J. C.: Landfast sea ice breakouts: Stabilizing ice features, oceanic and atmospheric forcing at Barrow, Alaska, *Continental Shelf Research*, 126, 10.1016/j.csr.2016.07.015, 2016.

Mahoney, A., Eicken, H., Gaylord, A. G., and Gens, R.: Landfast sea ice extent in the Chukchi and Beaufort Seas: The annual cycle and decadal variability, *Cold Reg Sci Technol*, 103, 41-56, 10.1016/J.Coldregions.2014.03.003, 2014.

Meyer, F. J., Mahoney, A. R., Eicken, H., Denny, C. L., Druckenmiller, H. C., and Hendricks, S.: Mapping arctic landfast ice extent using L-band synthetic aperture radar interferometry, *Remote Sens Environ*, 115, 3029-3043, 10.1016/J.Rse.2011.06.006, 2011.

Rampal, P., Weiss, J., and Marsan, D.: Positive trend in the mean speed and deformation rate of Arctic sea ice, 1979–2007, *Journal of Geophysical Research: Oceans*, 114, 10.1029/2008JC005066, 2009.

Spren, G., Kwok, R., and Menemenlis, D.: Trends in Arctic sea ice drift and role of wind forcing: 1992–2009, *Geophys Res Lett*, 38, 2011.

Stephenson, S. R., Smith, L. C., and Agnew, J. A.: Divergent long-term trajectories of human access to the Arctic, *Nat Clim Change*, 1, 156-160, 10.1038/Nclimate1120, 2011.

Werner, C., Wiesmann, A., Strozzi, T., Kos, A., Caduff, R., and Wegmüller, U.: The GPRI multi-mode differential interferometric radar for ground-based observations, *EUSAR 2012; 9th European Conference on Synthetic Aperture Radar*, 2012, 304-307

Zhang, J., Thomas, D., Rothrock, D., Lindsay, R., Yu, Y., and Kwok, R.: Assimilation of ice motion observations and comparisons with submarine ice thickness data, *Journal of Geophysical Research: Oceans*, 108, 2003.